to charge carrier, n.

$$\sigma \propto P_{O_2}^{-1/4} \quad (7)$$

The calculated exponent $-1/4$ based on the $V_O^{\cdot\cdot}$ and electron model is consistent with the experimental value. It is suggested that the possible defect in MgO-doped α-Nb_2O_5 systems be $V_O^{\cdot\cdot}$ and the electrical conduction occur through migration of electron. The fact that the electrical conductivity decreases with increasing mol% of MgO, as shown in Figure 6 means that the doubly ionized oxygen vacancy formed in equilibrium (1) moves the equilibrium (2) toward left-hand side. Therefore, MgO doping reduces the charge carrier concentration and so electrical conductivity.

Acknowledgement. The Present Studies were Supported by the Basic Science Research Institute program, Ministry of Education, 1989.

References

1. F. Holtzberg, A. Reisman, M. Berry, and M. Berkenbilt, *J. Amer. Chem. Soc.*, **79**, 2039 (1957).
2. L. K. Frevel and H. N. Rinn, *Anal. Chem.*, **27**, 1329 (1955).
3. B. M. Gatehouse and A. D. Wadsley, *Acta Cryst.*, **17**, 1545 (1964).
4. J. Yahia, *J. Chem. Phys. Solids*, **25**, 881 (1964).
5. A. A. McConnel, J. S. Anderson, and C. N. R. Rao, *Spectrochim. Acta*, **324**, 1067 (1976).
6. U. Balachandran and N. G. Eror, *J. Mater. Sci. Lett.*, **1**(9), 374 (1982).
7. N. T. McDevitt and W. L. Baun, *Spectrochim Acta*, **20**, 799 (1964).
8. G. Brauer, *Z. Anorg. Allem. Chem.*, **248**, 1 (1941).
9. P. Kofstad and P. B. Anderson, *J. Phys. Chem. Solids*, **21**, 280 (1961).
10. R. N. Blumenthal, J. B. Moser, and D. H. Whitmore, *J. Am. Ceram. Soc*, **48**, 617 (1965).
11. H. Schäfer, D. Bergner, and R. Gruehn, *Z. Anorg. Allgem. Chem.*, **365**, 31 (1969).
12. U. Balanchandran and N. G. Eror, *J. Mater. Sci.*, **17**, 1286 (1982).
13. P. Kofstad, "*Nonstoichiometry, Diffusion and Electrical Conductivity in Binary Metal Oxides*", Wiley-Interscience, New York, 1972, p. 188.
14. H. Kling, "*The Technology of Columbium*", John Wiley & Sons, New York, 1958, p. 87.
15. E. H. Greener, D. H. Whitmore, and M. E. Fine, *J. Chem. Phys.*, **34**, 1017 (1961).
16. P. Kofstad, *J. Chem. Phys.*, **23**, 1571 (1962).
17. R. Elo, R. A. Swalin, and W. K. Chen, *J. Chem. Phys. Solids*, **28**, 1625 (1967).
18. L. B. Valdes, *Proc. IRE*, **42**, 420 (1954).
19. J. T. Houghton and S. D. Smith, "*Infra-Red Physics*", Oxford University Press, G. B., 1966, p. 108.

Substitution Effect of Fluorine on $HoBa_2Cu_3O_{7-x}F_y$ ($0.0 \leq y \leq 0.5$) Superconductors

Jong Sik Park, Seong Han Kim, Hong Seok Kim, Seung Koo Cho, and Keu Hong Kim*

Department of Chemistry, Yonsei University, Seoul 120-749. *Received August 16, 1991*

High-Tc superconducting materials, $HoBa_2Cu_3O_{7-x}F_y$ with $0.0 \leq y \leq 0.5$, were synthesized by ceramic method and studied by X-ray diffraction, thermogravimetric analysis, differential thermal analysis, scanning electron microscopy and resistivity measurement. From the X-ray diffraction data, it was found that the samples had only single phase of which lattice volumes were decreased in proportional to the amount of fluorine, which indicated that the relatively small fluorine atoms are effectively substituted for the oxygen sites. Also, an anomalous phenomenon appeared that the peak intensites of (001) planes were greatly increased as fluorine contents increased. SEM photographs revealed that the grain sizes were enlarged progressively with fluorine contents. This fact could be explained along with DTA & TGA data that the incoporation of fluorine gave rise to lowering the melting point. Tc decreased as the incorporation of fluorine content increased. This implies that the superconducting electrons are perturbed due to the substitution of electronegative fluorine atom.

Introduction

Since the discovery of $YBa_2Cu_3O_{7-x}$ (YBCO) superconductor[1] with Tc more than 90 K, lots of experiments[2-5] were carried out to search for the doping effect of the impurity-substituted YBCO superconductors. Based on these experimental results, the doping effect of impurities on superconductivity and structural changes induced from substitutions are helpful to lighten the high-Tc superconducting mechanism which is not well known yet.

Baetzold[6] peported that when the ferromagnetic rare-earth metal ions such that La^{3+}, Nd^{3+}, Eu^{3+}, Gd^{3+}, Ho^{3+}, Er^{3+} and Lu^{3+} were substituted for Y^{3+} sites of YBCO, no dramatic changes in physical properties could occur. Ho *et al.*[7] explained from these results that there were no interactions between spins of the ferromagnetic elements substituted in

YBCO and of the superconducting electrons. Tarascon *et al.*[8] reported that Tc decreased when the Ba^{2+} sites were substituted with other cations having 2+ oxidation state such that Sr^{2+}. This is due to the perturbation of Cu-O network resulted from the substituted cations. Baetzold[6], also, reported that Ni^{2+}, Zn^{2+} and Cd^{2+} ions prefered to substitute the Cu(2) sites and Al^{3+}, Fe^{3+} and Ga^{3+} ions prefered to do the Cu(1) sites. However, the substitution of transition metal ions or other cations for Cu^{2+} sites decreases Tc. Ovshinsky *et al.*[9] and Tyagi *et al.*[10] published that the substitution for the O^{2-} sites of anions such as S^{2-}, Cl^{-}, Te^{2-} and Se^{2-} caused to change the physical properties. Kim *et al.*[11] concluded from the results of thermopower measurements and micro-Raman spectroscopy that the fluorinated YBCO system in which O^{2-} was substituted with F^{-} had the tendency of preferential subsitution for pyramidal Cu-O units rather than for Cu-O chains. From the above results, it is concluded that Y^{3+} and Ba^{2+} do not have key roles on the superconductivity, but serves only the linking of copper-oxygen network, and Cu^{2+} and O^{2-} have important roles.

In this work, we substituted the oxygen sites in $HoBa_2Cu_3O_{7-x}$ (Ho123) with fluorine atoms and measured the various physical properties, which were expected to be helpful to search for the roles of pyramidal Cu-O networks on high-Tc superconductivity.

Experimental

Sample Synthesis and Analysis. In order to synthesize high-Tc superconductor, $HoBa_2Cu_3O_{7-x}F_y$ system with $y=0.0$, 0.1, 0.2, 0.3, 0.4 and 0.5, we used Ho_2O_3 (99%, Aldrich Co.), $BaCO_3$ (99%, Hayashi Chemicals Ltd.), CuO (99.9%, Fluka Co.) and CuF_2 (99.9%, Aldrich Co.) as starting materials. These mixtures with appropriate compositions were accurately weighed, well ground in an agate mortar using ethanol, and calcined at 800℃ for 24 h to remove CO_2 and H_2O. The powders were made into pellets under a pressure of 49 MPa, and then sintered at 930℃ for 48 h. The pellets were annealed at 750℃ for 24 h to control the oxygen contents, followed by cooling to 300℃ at the rate of 50℃/h.

X-ray diffraction (XRD), scanning electron microscopy (SEM) and thermal analysis (DTA/TGA) were carried out to characterize the samples. XRD analysis was undertaken using Philips PW 1710 diffractometer with CuKα as a light source and graphite monochromator in the 2θ range of 5-80°. From the XRD results, the crystal structure, lattice parameter and unit cell volume could be obtained. SEM and thermal analysis were carried out using Hitachi S-510 and Rigaku PTC-10 AC (CN 8078 B1) with heating rate of 5℃/min in air, respectively. TGA and DTA range were 20.0 mg and ± 100 μV, respectively.

Resistivity Measurements. After each pellet was patterned to square disk with 2.0 mm×4.0 mm×10.0 mm, the resistivity was measured by standard four-probe a.c. method. Copper wire as electrode was contacted by indium. Temperature was measured by copper-constantan thermocouple setting beside the sample, using PCLD 789 MUX multiplexer board (Advantech Co., Ltd.) with the error range of ± 0.01℃. The resistivity was measured by lock-in amplifier (EG & G Co., PARC 5210) with the current, frequency and voltage fixed at 5-10 mA, 110 Hz and 10 μV, respectively. The output of lock-in amplifier and temperature were simultaneously recorded by PCL 714 14-bit A/D convert (Advantech Co., Ltd.) and computer.

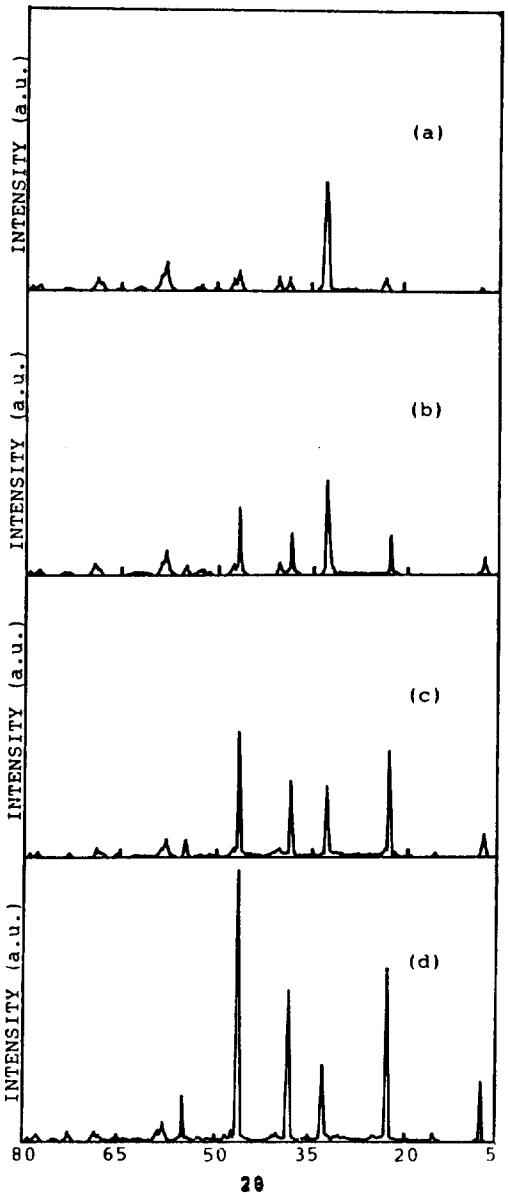

Figure 1. XRD patterns of $HoBa_2Cu_3O_{7-x}F_y$ system. (a) $y=0.0$, (b) $y=0.1$, (c) $y=0.3$ and (d) $y=0.5$.

Results and Discussion

The X-ray diffraction data and their indexing of $HoBa_2Cu_3O_{7-x}F_y$ system were shown in Figure 1 and Table 1, respectively and d (cal) was obtained by least square method. From these results, it was found that pure Ho123 and fluorinated Ho123 had single phase with orthorhombic structure, and the peak intensities corresponding to (001) planes graduaHy increased dramatically with the amount of fluorine, compared to the intensity of (103) plane which shows a maximum in pure Ho123. The increase of intensities of (001) peaks was reported in the case of YBCO thin film[12] where the particles had the c-axis orientation and in the case of molten-oxide

Table 1. Indexation of XRD Spectra for the $HoBa_2Cu_3O_{7-x}$ and $HoBa_2Cu_3O_{7-x}F_{0.5}$

	$HoBa_2Cu_3O_{7-x}$			$HoBa_2Cu_3O_{7-x}F_{0.5}$		
h k l	*d* (obs)	*d* (cal)	I/I_0	*d* (obs)	*d* (cal)	I/I_0
0 0 1	--	–	–	11.7422	11.6790	96
0 0 2	--	–	–	5.8384	5.8395	13
0 0 3	3.8963	3.8952	18	3.8901	3.8930	296
0 0 4	--	–	–	2.9261	2.9198	13
1 0 3	2.7429	2.7314	100	2.7413	2.7265	100
0 0 5	2.3263	2.3371	12	2.3359	2.3358	257
1 1 3	2.2424	2.2372	13	2.2307	2.2328	17
0 0 6	1.9482	1.9476	25	1.9468	1.9465	435
2 0 0	1.9145	1.9156	18	1.9090	1.9099	22
0 0 7	--	–	–	1.6690	1.6684	74
1 2 3	1.5848	1.5870	30	1.5861	1.5836	30
2 1 3	1.5731	1.5729	17	1.5679	1.5690	13
0 2 6	1.3791	1.3780	7	–	–	–
1 0 8	1.3648	1.3649	18	1.3646	1.3668	22
0 0 9	--	–	–	1.2987	1.2977	22
0 3 3	--	–	–	1.2302	1.2304	13

Table 2. Cell Parameters for Various Samples with Orthorhombic Systems

Samples	a(Å)	b(Å)	c(Å)
$HoBa_2Cu_3O_{7-x}$	3.831	3.900	11.686
$HoBa_2Cu_3O_{7-x}F_{0.1}$	3.831	3.893	11.689
$HoBa_2Cu_3O_{7-x}F_{0.2}$	3.823	3.895	11.693
$HoBa_2Cu_3O_{7-x}F_{0.3}$	3.821	3.894	11.689
$HoBa_2Cu_3O_{7-x}F_{0.4}$	3.820	3.889	11.688
$HoBa_2Cu_3O_{7-x}F_{0.5}$	3.820	3.891	11.679

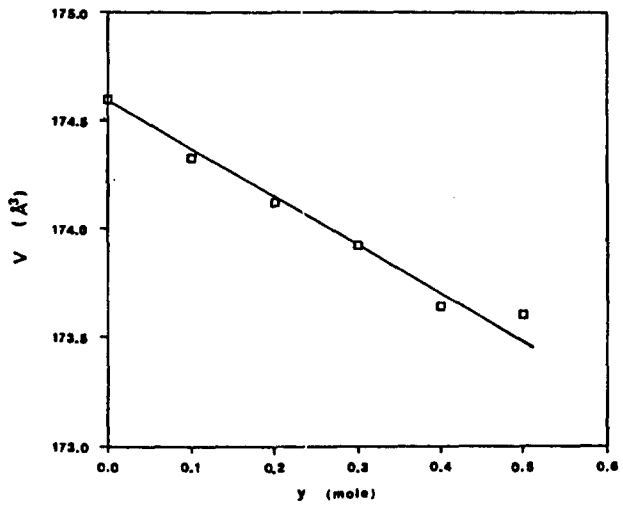

Figure 2. The unit cell volume (V) *vs.* fluorine content for $HoBa_2Cu_3O_{7-x}F_y$ system.

process which reported by Jin *et al.*[13] in which niddle-shaped grains were aligned along c-axis due to melt-textured growth. But, in our case, the powder consists of niddle-shape particles as shown in Figures 4 and 5, and these tend to become

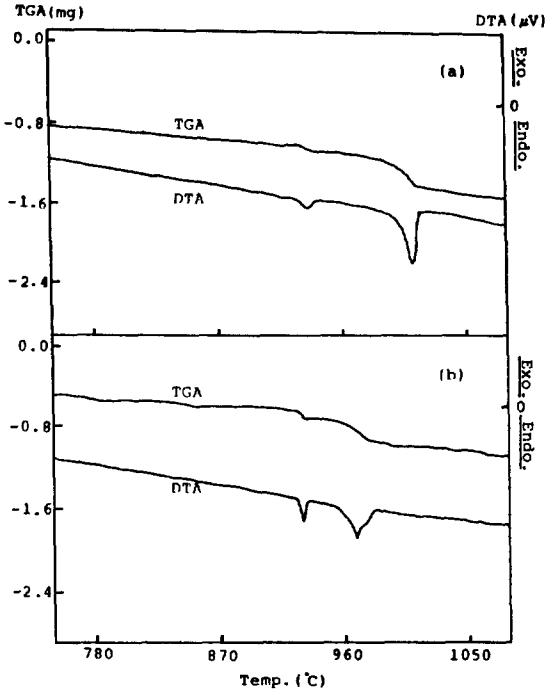

Figure 3. DTA and TGA curves for (a) $HoBa_2Cu_3O_{7-x}$ and (b) $HoBa_2Cu_3O_{7-x}F_{0.5}$.

aligned parallel to the specimen axis in the preparation of the sample for XRD[14]. Therefore, this causes an intensification of the (001) peaks, and a weakening of them elsewhere.

Table 2 and Figure 2 show the lattice parameters calculated from the XRD patterns and the unit cell volume corresponding to each sample, respectively. The lattice parameters and unit cell volume decrease gradually in the proportion to the amount of fluorine. This is considered to be due to the substitution of small-size fluorine atom (119 pm) for the relatively large oxygen atom (126 pm)[15].

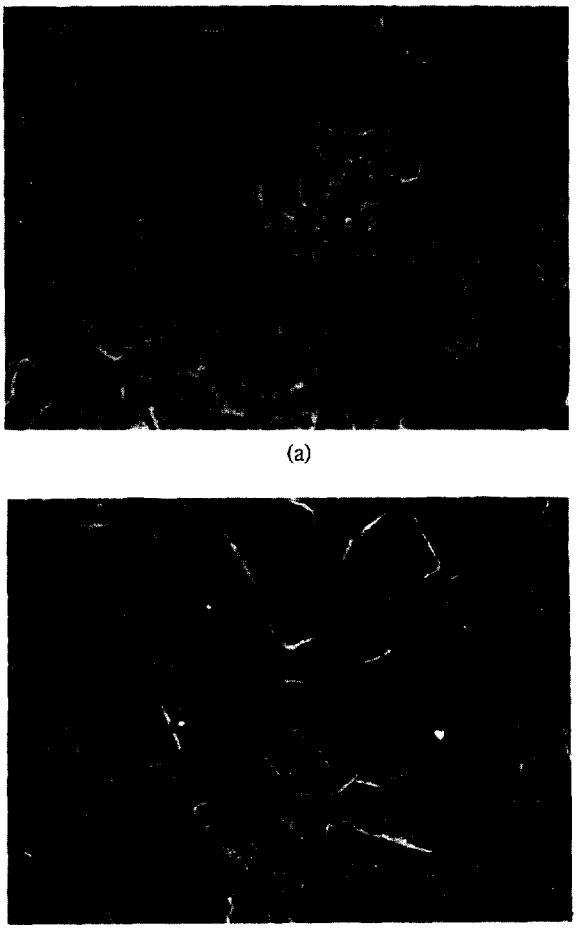

Figure 4. SEM photographs of (a) $HoBa_2Cu_3O_{7-x}$ (×2000) and (b) $HoBa_2Cu_3O_{7-x}F_{0.1}$ (×2000).

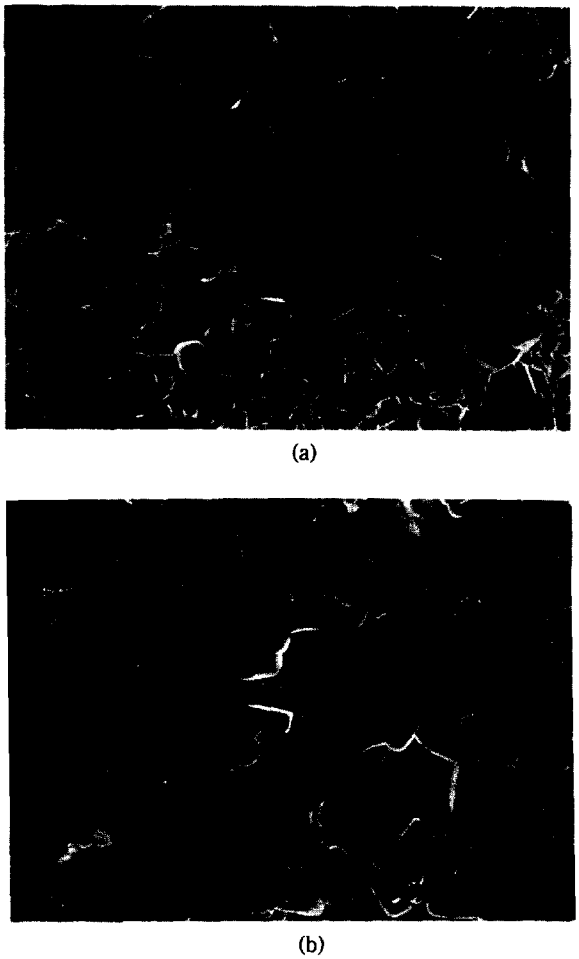

Figure 5. SEM photographs of (a) $HoBa_2Cu_3O_{7-x}F_{0.3}$ (×900) and (b) $HoBa_2Cu_3O_{7-x}F_{0.5}$ (×900).

Figure 3 shows DTA/TGA for pure and fluorinated Ho123 superconductors. As shown in Figure 3(a), pure Ho123 has two peaks; one small endothermic peak at 930℃ accompanied with few weight loss corresponds to the phase transition to Ho123 superconductor and the other larger endothermic peak at 1000℃ is due to the decomposition of $2HoBa_2Cu_3O_{7-x}$ into Ho_2BaCuO_5 and the liquid phase of $3BaCuO_2$ and 2CuO, which is well agreed to the result reported by Murakami *et al.*[16] on the basis of computer-assisted electron probe microanalysis. In the case of $HoBa_2Cu_3O_{7-x}F_{0.5}$ shown in Figure 3(b), the phase transition peak to superconductor phase is coincident with that of pure Ho123; but the decomposition peak is shifted to about 960℃. The depression of the decomposition temperature to Ho_2BaCuO_5 and liquid phase is regarded as the formation of eutectic mixture with substituted fluorine.

SEM photographs of pure and fluorinated Ho123 samples are shown in Figures 4 and 5. The grain sizes of the fluorinated samples increase with the amount of fluorine. This phenomenon is explained by the DTA results. The thermal fluctuation in the furnace could repeatedly cause partial melting and recrystallization of the sample, which affects more seriously to the case of the narrow temperature range between phase transition and melt decomposition, resulting into the grain growth.

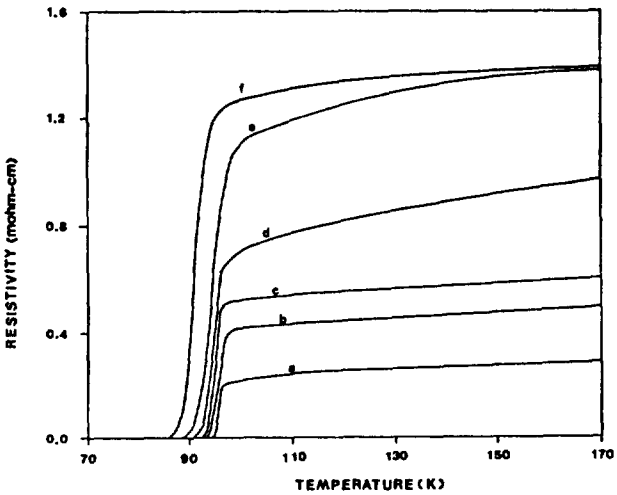

Figure 6. Resistivity *vs.* temperature for $HoBa_2Cu_3O_{7-x}F_y$ system. (a) $y=0.0$ T_c: 94.3 K, (b) $y=0.1$ T_c: 93.2 K, (c) $y=0.2$ T_c: 92.6 K, (d) $y=0.3$ T_c: 90.4 K, (e) $y=0.4$ T_c: 88.5 K and (f) $y=0.5$ T_c: 86.2 K.

Figure 6 shows the electrical resistivity of the $HoBa_2Cu_3O_{7-x}F_y$ system as a function of temperature. In YBCO struc-

ture, the combination of Cu and Ba allows the conduction band to have a large oxygen component with strong coupling between metal *d* electrons and oxygen displacement[17]. Since the fluorine atom has lower 2*p* level in energy, it deteriorates the conduction band due to weaker overlap between Cu *d* orbital and F 2*p* orbitals. Therefore, Tc decreases with the substitution of fluorine.

In summary, the incorporation of fluorine atom into $HoBa_2Cu_3O_{7-x}$ results in the increase of the (001) peaks in the XRD spectra of which the reason is not clarified, the decrease of the unit cell volume, the increase of the grain size, and the decrease of Tc due to the perturbation of electron.

Acknowledgement. The financial support of the Ministry of Science and Technology is greatly acknowledged. The authors are also thankful from the assistance of the SEM analysis by Mr. J. S. Hwang and DTA/TGA by D. Y. Lee.

References

1. M. K. Wu, J. R. Ashbun, C. J. Torng, P. H. Hor, R. L. Meng, L. Gao, Z. J. Huang, Y. Q. Wang, and C. W. Chu, *Phys. Rev. Lett.*, **58**, 908 (1987).
2. M. S. Islam and R. C. Baetzold, *Phys. Rev.*, **B40**(16), 926 (1989).
3. H. L. P. Youn, A. E. Dwight, J. L. Matykiewicz, and C. W. Kimball, *Phys. Lett.*, **140**, 75 (1989).
4. Y. Morioka, A. Tokiwa, M. Kikuchi, and Y. Syono, *Solid State Commun.*, **67**(3), 267 (1988).
5. C. Rettori, D. Davidov, I. Belaish, and I. Felner, *Phys. Rev.*, **B36**(7), 4028 (1987).
6. R. C. Baetzold, *Phys. Rev.*, **B38**(16), 304 (1988).
7. J. C. Ho, P. H. Hor, R. L. Meng, C. W. Chu, and C. Y. Huang, *Solid State Commun*, **63**, 711 (1987).
8. T. M. Tarascon, L. H. Greene, B. G. Bagley, W. R. McKinnon, P. Barboux, and G. W. Hull, "Novel Superconductivity", ed. by S. A. Wolf and V. Z., Kresin Plenum, N. Y., p. 705-274 (1987).
9. S. R. Ovshinsky, R. T. Young, D. D. Allred, G. DeMaggio, and Van der Leeden G. A., *Phys. Rev. Lett.*, **58**(24), 2579 (1987).
10. A. K. Tyagi, S. J. Patwe, U. R. K. Rao, and R. M. Iyer, *Solid State Commun.*, **65**(10), 1149 (1988).
11. K. H. Kim, D. Kim, S. K. Cho, Y. W. Choi, J. S. Park, and J. S. Choi, *Bull. Korean Chem. Soc.*, **11**(3), 191 (1990).
12. M. Kawasaki, S. Nakata, Y. Sato, M. Funabashi, T. Hasegawa, K. Kishio, K. Kitazawa, K. Fueki, and H. Koinuma, *Jpn. J. Appl. Phys.*, **26**(5), L738 (1987).
13. S. Jin, T. H. Tiefel, R. C. Sherwood, R. B. van Dover, M. E. Davis, G. W. Kammlott, and R. A. Fastnacht, *Phys. Rev.*, **B37**, 7850 (1988).
14. L. V. Azaroff and M. J. Buerger, "The Powder Method in X-ray Crystallography", McGraw-Hill, N. Y., pp. 258 (1958).
15. J. E., Huheey, "Inorganic Chemistry", Happer, Cambridge, 3rd Ed., pp. 73-74 (1983).
16. M. Murakami, M. Morita, K. Doi, K. Miyamoto, and H. Hamada, *Jpn. J. Appl. Phys.*, **28**(3), L399 (1989).
17. M. O'Keeffe and S. Hansen, *J. Am. Chem. Soc.*, **110**, 1506 (1988).

Oxidative Addition Reaction of Mono(ary)cyanoplatinum(II) Complex with Two Amino Ligands with the Dihalogens

Jaejung Ko*, Moonsik Kim, Seho Kim, and Yookil Shin

Department of Chemical Education, Korea National University of Education, Chungbuk 363-791

Received September 4, 1991

The mono(aryl)cyanoplatinum(II) complex $[Pt(CN)(C_6H_3\{CH_2NMe_2\}_2\text{-}2,6)]$ reacts with the dihalogens to yield the mono (aryl)cyanoplatinum complexes $[PtX_2(CN)(C_6H_3\{CH_2NMe_2\}_2\text{-}2,6)]$ (X=Cl, Br, I). The structural configuration of the two halogen atoms for a square planar platinum complex was studied by ^{1}H-NMR spectroscopy and led to a mixture of *trans* and *cis* orientation. The *trans* orientation was found to be more stable in energy (1.33 kcal/mol) than the *cis* orientation by means of Extended Hückel calculations. On the base of a combination of the analysis of ^{1}H-NMR, ^{13}C-NMR spectra and computational calculations it is assumed that the intermediate consists of an initial attack in the linear transition state, leading to the S_N2 type mechanism.

Introduction

Oxidative addition reaction is of remarkable importance, since nearly all catalytic and many useful stoichiometric processes involve oxidative addition reation[1]. Recently, Rund and coworkers[2] reported the oxidative addition reaction of dihalogens to $(TBA)_2Pt(CN)_4$, leading to *trans* $(TBA)_2Pt(CN)_4X_2$ products. They suggested that the oxidative addition reactions presumably proceed with linear transition state (a) rather than three centered transition state (b), as shown below, leading to *trans*-X_2 arrangements in the product. In recent years, Koten and coworkers[3] also reported the oxidative addition reactions of dihalogens to square planar platinum (II) complexes. They also concluded that when steric factors preve-